

Adhesively bonded Ce:YIG/SOI integrated optical circulator

Samir Ghosh,^{1,2,*} Shahram Keyvaninia,^{1,2} Wim Van Roy,³ Tetsuya Mizumoto,⁴
Gunther Roelkens,^{1,2} and Roel Baets^{1,2}

¹Photonics Research Group, Department of Information Technology (INTEC), Ghent University, Sint-Pietersnieuwstraat 41, Gent 9000, Belgium

²Center for Nano- and Biophotonics (NB-Photonics), Ghent University, Sint-Pietersnieuwstraat 41, Gent 9000, Belgium

³Functional Nanosystems, Interuniversity Microelectronics Center (IMEC), Kapeldreef 75, Heverlee B-3001, Belgium

⁴Department of Electrical and Electronic Engineering, Tokyo Institute of Technology, 2-12-1 Ookayama, Meguro-ku, Tokyo 152-8552, Japan

*Corresponding author: samir.ghosh@intec.ugent.be

Received January 18, 2013; accepted January 28, 2013;
posted February 11, 2013 (Doc. ID 183811); published March 14, 2013

A classical 3-port optical circulator is demonstrated on the silicon-on-insulator (SOI) platform. A garnet die with a magneto-optical cerium-doped yttrium iron garnet (Ce:YIG) layer is bonded on top of a Mach-Zehnder interferometer circuit using a thin adhesive bonding layer. The power transmission between different ports is characterized in the presence of an external magnetic field, transversal to the light propagation direction. An isolation of 22 dB is measured at a wavelength of 1562 nm. © 2013 Optical Society of America

OCIS codes: 130.3120, 230.3810.

In recent years the silicon-on-insulator (SOI) platform has become a promising technology for highly integrated photonic circuits by virtue of the high index contrast between the silicon waveguide core and the SiO₂ cladding. Many types of optical components have been studied in great detail on the SOI platform except for isolators and circulators. To achieve a highly functional photonic integrated circuit, on-chip nonreciprocal devices, such as optical circulators and isolators are highly desirable. A circulator is a three or 4-port device in which light circulates in a particular direction, which is an interesting functionality in a myriad of applications. Currently, commercially available optical circulators are built by configuring several bulk optical components, such as Faraday rotators, polarization beam splitters and half-wave plates. To miniaturize the circulator to an on-chip version different endeavors are already reported with device lengths ranging from a few wavelengths [1,2] to hundreds of wavelengths [3,4]. A theoretical study of resonator-type circulators in which clockwise (CW) and counter clockwise (CCW) modes of propagations experience a different phase velocity due to the influence of a magnetic field on the optical mode in the waveguide has been reported [5]. Resonator-based circulators inherently suffer from narrow band operation. A waveguide-based Mach-Zehnder interferometer (MZI) type optical circulator exploiting nonreciprocal phase shift (NRPS) was also investigated almost two decades ago [6]. 3-port or 4-port circulators can be considered as extensions of 2-port isolators. The nonreciprocal effect can be achieved by introducing a magnetic medium in the light path. A straightforward way to integrate a magnetic medium with a silicon optical waveguide circuit is by bonding a die of ferromagnetic/ferrimagnetic material on top of the waveguide as recently demonstrated [7–9]. Alternatively, the sputter deposition of such magnetic material directly on top of silicon waveguides has been reported [10].

In this work an SOI-based MZI of size 3.7 mm × 1 mm is used in which a 4 mm² garnet die consisting of a

300 nm thin cerium-doped yttrium iron garnet (Ce:YIG) layer on a 450 μm thick substituted gadolinium gallium garnet (SGGG) substrate is adhesively bonded partially on top of the interferometer arms with the help of a benzocyclobutene (BCB) bonding agent. The bonding procedure can be found in [7,11]. The interferometer structure, implemented in a 220 nm thick silicon device layer on a 2 μm thick buried oxide layer is depicted in Fig. 1. Two 2 × 2 directional couplers are connected by 900 nm wide silicon waveguides to construct the 3-port MZI. The directional couplers are designed for having BCB as the top cladding. One of the outputs of the directional coupler 2 is looped by a 1 × 2 multimode interferometer (MMI) to make the device a 3-port. This 1 × 2 MMI is also designed for BCB top cladding. The length and width of the 1 × 2 MMI is designed as 10.5 and 4.0 μm, respectively. The length of the nonreciprocal phase shifter is designed as 1.6 mm in each arm which is sufficient for a NRPS of π/2 between forward and backward directions as mentioned in [7] for a BCB thickness of 100 nm between the silicon waveguide and the Ce:YIG layer. Noteworthy to mention here is that the device works in push-pull when a unidirectional magnetic

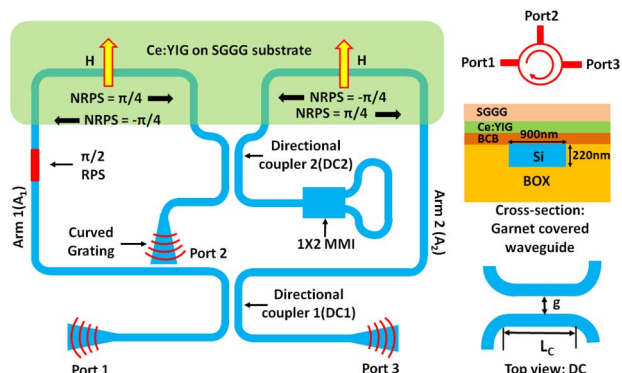


Fig. 1. (Color online) Schematic diagram of garnet bonded 3-port MZI type optical circulator.

Table 1. Total Phases at Final Ports without Loop Path^a

Path	Arm	RP	NRP	ϕ	C/D
1 → 2	A ₁	$\pi/2$	$\pi/4$	$3\pi/4$	C
1 → 2	A ₂	π	$-\pi/4$	$3\pi/4$	
2 → 1	A ₁	$\pi/2$	$-\pi/4$	$\pi/4$	D
2 → 1	A ₂	π	$\pi/4$	$5\pi/4$	
2 → 3	A ₁	π	$-\pi/4$	$3\pi/4$	C
2 → 3	A ₂	$\pi/2$	$\pi/4$	$3\pi/4$	
3 → 2	A ₁	π	$\pi/4$	$5\pi/4$	D
3 → 2	A ₂	$\pi/2$	$-\pi/4$	$\pi/4$	

^aC/D—constructive/destructive interference.

field is applied transverse to the light propagation direction in the Ce:YIG covered sections.

The operation of the circuit as a 3-port circulator can be explained by considering the structure in Fig. 1 as broadband device containing a $\pi/2$ reciprocal phase shifter (RPS) on one of the arms (say arm 1). The light propagating between 2-ports in a particular direction experiences different phases while passing through directional couplers, RPS and nonreciprocal phase shifters of the circuit. The overall phases (besides a trivial constant factor which is the same for both arms) at all 3-ports for both the forward and backward directions are summarized in Tables 1 and 2. A 90 deg reciprocal phase shift for the cross-coupling in the directional coupler is assumed whereas 0 deg is assumed for the bar coupling. The phases for light transmission between ports 1 and 3 are tabulated separately in Table 2 because the reflected light at the loop takes two paths after splitting at DC2. RP is the total reciprocal phase accumulated by light traveling through any of the paths whereas NRP is the nonreciprocal phase provided by the MZI arm with magnetic field transverse to the light propagation direction. The arrow in the “Path” column indicates the direction of light flow. L in Table 2 is used to abbreviate the loop way created by the 1×2 MMI. Here ϕ means the sum of RP and NRP.

It can be observed that for one particular direction in which light is flowing between ports (as shown in Fig. 1) constructive interference is obtained, while in the opposite direction destructive interference is obtained. Hence the circuit works as a 3-port circulator.

A 2D full-vectorial finite difference method is adopted for the design of the required directional couplers. The waveguide width and thickness are 900 and 220 nm, respectively. The gap (g) between the waveguides is 250 nm in the 12 μm long coupling section.

Table 2. Total Phases at Final Ports with Loop Path

Path	RP	NRP	ϕ	C/D
1 → A ₁ → L → A ₁ → 3	$5\pi/2$	0	$5\pi/2$	D
1 → A ₁ → L → A ₂ → 3	π	$\pi/2$	$3\pi/2$	
1 → A ₂ → L → A ₁ → 3	2π	$-\pi/2$	$3\pi/2$	
1 → A ₂ → L → A ₂ → 3	$\pi/2$	0	$\pi/2$	
3 → A ₁ → L → A ₁ → 1	$5\pi/2$	0	$5\pi/2$	C
3 → A ₁ → L → A ₂ → 1	2π	$\pi/2$	$5\pi/2$	
3 → A ₂ → L → A ₁ → 1	π	$-\pi/2$	$\pi/2$	
3 → A ₂ → L → A ₂ → 1	$\pi/2$	0	$\pi/2$	

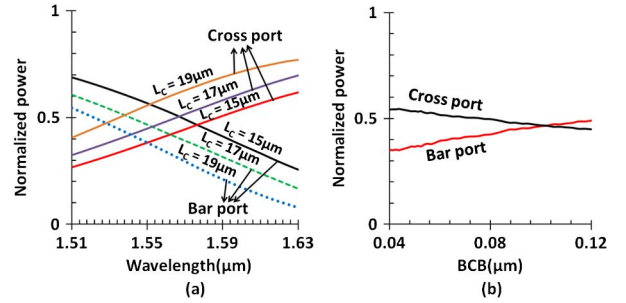


Fig. 2. (Color online) Coupling efficiency of the bar and cross ports of the directional coupler (a) as a function of wavelength, with a gap of 250 and 100 nm BCB thickness for various coupler lengths (L_c) and (b) as a function of BCB thickness for $L_c = 15 \mu\text{m}$, gap = 250 nm at 1.577 μm wavelength.

Taking into account the bent entrance and exit waveguides an effective coupling length L_c of 15 μm is considered. The performance of the directional coupler depends on the operating wavelength as shown in Fig. 2(a). The BCB thickness is taken as 100 nm on top of the waveguides although the actual BCB thickness does influence the directional coupler's performance much as depicted in Fig. 2(b). Transverse magnetic (TM)-polarized light is assumed in the simulation, since the NRPS is only observed for this polarization. From Fig. 2(a) we can see that the 3 dB coupling length is varying with wavelength. For our current designed device with $L_c = 15 \mu\text{m}$ the optimum operating wavelength range lies between 1.56 and 1.58 μm . The circuit depicted in Fig. 1 behaves as a broadband circulator but for that a perfect alignment of the garnet die on the MZI arms is required so that there is no extra RPS created between both arms of the MZI. In the real device there was no extra $\pi/2$ RPS, rather it was designed to be perfectly symmetric and the garnet die was intentionally bonded slightly tilted as to provide difference in optical path length between both arms, thereby also making the isolator wavelength dependent and hence less broadband.

As the TM mode can only experience NRPS in this configuration, TM curved grating couplers were used to inject and collect light from the respective ports [12]. A stack of three miniature Nd-B-Fe magnets are used to bias the ferrimagnetic Ce:YIG layer. Input and output fibers are swapped while the magnet orientation is kept fixed during the measurements. The power transmission results are shown in Figs. 3(a) and 3(b) for CCW and CW propagation through the circulator, respectively. Power transmissions between all combination of ports at 1573 nm are shown in Table 3.

It is important to mention that all the six measurements were not obtained simultaneously because of the setup constraints and for each set of measurements the magnet-stack needed to be moved while keeping the direction of magnetic field unaltered. This resulted in a small offset of the wavelengths at which perfect constructive and destructive interference occurred. The average free spectral range of 20 nm implies that the difference in garnet covered lengths in both the arms is about 135 μm as the mean group index of garnet and BCB clad waveguide differs from only from that of the

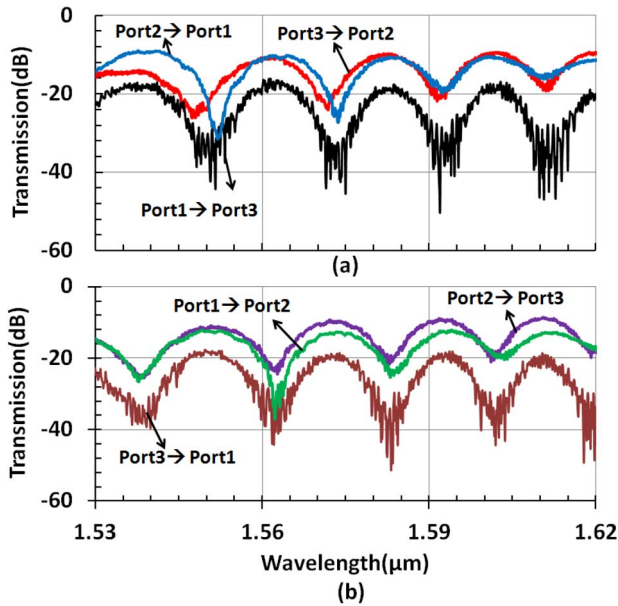


Fig. 3. (Color online) Measured optical transmission spectra at different ports of the circulator under a constant magnetic field (a) CCW and (b) CW.

Table 3. Measured Transmissions (T) at 1573 nm

Ports	T (dB)	Ports	T (dB)
1 \rightarrow 2	-13	2 \rightarrow 1	-22
2 \rightarrow 3	-9	3 \rightarrow 2	-20
3 \rightarrow 1	-19	1 \rightarrow 3	-32

BCB clad waveguide by 0.92 in the 1.54–1.60 μm wavelength range. A maximum isolation of 22 dB is observed between ports 1 and 2 at a wavelength of 1562 nm. Perfectly balanced splitters would result in an even higher optical isolation. The power transmission levels between ports 1 and 3 are about 8 dB less compared to other ports because of the double path length traversed by the light after reflecting back from the 1×2 MMI including 0.5 dB loss due to the MMI. The total insertion loss for the transmission between ports 1 and 2 or ports 2 and 3 is about 10 dB which is consistent with the value reported in [7]. The performance of the reference directional couplers are also characterized separately which are assumed to have been covered by 100 nm BCB thickness as shown in Fig. 4. The trend shown in Fig. 2 also corresponds to the measured values presented in Fig. 4.

In conclusion, a 3-port circulator was demonstrated on the SOI platform using an adhesive BCB bonding

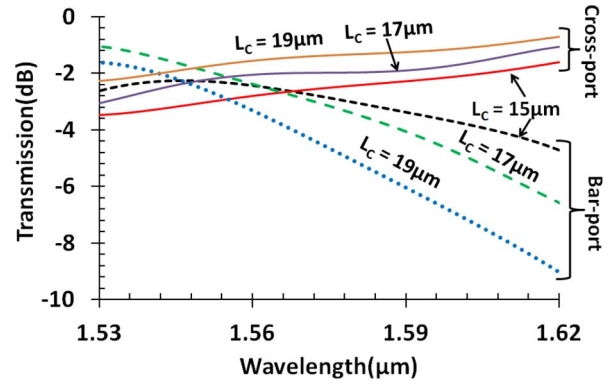


Fig. 4. (Color online) Measured optical transmission spectra at bar and cross ports of different reference directional couplers.

technique. While the performance and the insertion loss of the device can be improved, the demonstration provides a scope for the integration of circulators with other photonic components to achieve a fully functional photonic integrated circuit.

References

1. W. Zheng and S. Fan, *Opt. Lett.* **30**, 15 (2005).
2. W. Smigaj, J. R. Vivas, B. Glalak, L. Magdenko, B. Dagens, and M. Vanwollegham, *Opt. Lett.* **35**, 568 (2010).
3. M. Lohmeyer, S. Mikhail, and P. Hertel, *Opt. Eng.* **36**, 889 (1997).
4. N. Sugimoto, T. Shintaku, A. Tate, H. Terui, M. Shimokozono, E. Kubota, M. Ishii, and Y. Inoue, *IEEE Photon. Technol. Lett.* **11**, 355 (1999).
5. W. Zheng and S. Fan, *Appl. Phys. B* **81** 2 (2005).
6. T. Mizumoto, H. Chihara, N. Tokui, and Y. Naito, *Electron. Lett.* **26** 199 (1990).
7. S. Ghosh, S. Keyvavinia, W. Van Roy, T. Mizumoto, G. Roelkens, and R. Baets, *Opt. Express* **20** 1839 (2012).
8. S. Ghosh, S. Keyvavinia, W. Van Roy, T. Mizumoto, G. Roelkens, and R. Baets, *IEEE Photon. Technol. Lett.* **24**, 1653 (2012).
9. T. Mizumoto, Y. Shoji, and R. Takei, *Materials* **5**, 5 (2012).
10. L. Bi, J. Hu, P. Jiang, D. H. Kim, G. F. Dionne, L. C. Kimerling, and C. A. Ross, *Nat. Photonics* **5**, 758 (2011).
11. S. Keyvaninia, M. Muneeb, S. Stankovi, P. J. Van Veldhoven, D. Van Thourhout, and G. Roelkens, *Opt. Mater. Express* **3**, 35 (2013).
12. D. Vermeulen, K. Van Acoleyen, S. Ghosh, S. Selvaraja, W. A. D. De Cort, N. A. Yebo, E. Hallynck, K. De Vos, P. P. Debackere, P. Dumon, W. Bogaerts, G. Roelkens, D. Van Thourhout, and R. Baets, "Efficient tapering to the fundamental quasi-TM mode in asymmetrical waveguides," presented at *European Conference on Integrated Optics (ECIO)*, Cambridge, UK, April 6–9, 2010.